Coulomb and Liquid Dimer Models in Three Dimensions

David A. Huse,[1] Werner Krauth,[2] R. Moessner,[3] and S. L. Sondhi[1]

[1]*Department of Physics, Princeton University, Princeton, New Jersey 08544, USA*

[2]*CNRS-Laboratoire de Physique Statistique de l'Ecole Normale Supérieure, Paris, France*

[3] *Laboratoire de Physique Théorique de l'Ecole Normale Supérieure, CNRS-UMR8549, Paris, France*

(Received 21 May 2003; published 16 October 2003)

We study classical hard-core dimer models on three-dimensional lattices using analytical approaches and Monte Carlo simulations. On the bipartite cubic lattice, a local gauge field generalization of the height representation used on the square lattice predicts that the dimers are in a critical Coulomb phase with algebraic, dipolar correlations, in excellent agreement with our large-scale Monte Carlo simulations. The nonbipartite fcc and Fisher lattices lack such a representation, and we find that these models have both confined and exponentially deconfined but no critical phases. We conjecture that extended critical phases are realized only on bipartite lattices, even in higher dimensions.

DOI: 10.1103/PhysRevLett.91.167004 PACS numbers: 74.20.Mn, 05.50.+q, 75.10.Hk, 75.10.Jm

The statistical mechanics of dimers on a lattice that interact with one another only via hard-core exclusion has long been of interest to mathematicians and physicists [1,2]. It is one of the simplest models describing the arrangement of anisotropic objects on a regular substrate. Applications [3] range from diatomic molecules on surfaces to spin ice in a magnetic field [4].

By Kasteleyn's theorem, on two-dimensional (2D) planar lattices, the statistical mechanics of (close-packed) dimer coverings can be computed exactly [5]. A consistent picture has emerged from this work for a large class of 2D dimer models. On bipartite 2D lattices, dimer models are in confined phases in which the free energy of two inserted test monomers (unpaired sites) increases with separation. The increase is logarithmic for phases with algebraic dimer correlations and linear for the remaining ones. An example of the former is the square lattice [5,6] and one of the latter is the exotic diamond-octagon "4-8" lattice which exhibits two confining phases as the strength of the diamond bonds is varied [3]. By contrast, nonbipartite lattices exhibit both deconfined and confined phases but always with exponentially decaying dimer correlations except at the boundary between such phases. Examples are the triangular [7,8] and kagome [9] lattices, which are deconfined with exponentially decaying correlations, and the Fisher lattice—equivalent to the 2D Ising model [10]—which exhibits a deconfinement transition [11].

Dimer models on two-dimensional bipartite lattices can also be understood through their height representations [12,13]. Within this powerful framework, the two subcategories of critical and noncritical dimer correlations are described as "rough" and "flat" phases. In either case the defect interaction corresponding to the monomer free energy is long ranged. Dimer models on nonbipartite lattices lack a similar long-wavelength description.

In this Letter we generalize the height representation to three dimensions. We show that dimer models on bipartite 3D lattices admit a local gauge representation which results in a "Coulomb" phase with algebraic, dipolar forms for the dimer correlations and monomer interactions that fall off inversely with their separation. We present large-scale Monte Carlo simulations on 3D lattices and demonstrate that the dimer model on the cubic lattice is critical. On nonbipartite lattices we show that there exist both confined and deconfined phases, with exponentially decaying dimer correlations and monomer interactions, finding that the face-centered cubic (fcc) lattice and the 3D Fisher lattice realize these cases. As will be discussed elsewhere, the Coulomb and liquid phases can be identified with the U(1) and Z_2 deconfined phases [14] in the corresponding quantum dimer models [15].

We first report our results on the cubic lattice along with the gauge representation. Thereafter we consider the fcc and Fisher lattices and conclude with a summary and some conjectures on related models.

Cubic lattice.—Generally, for any dimer configuration, we define dimer numbers $\mathbf{n}(\mathbf{x})$ as $n_i(\mathbf{x}) = 1$ if the bond between sites $\mathbf{x}$ and $\mathbf{x} + \mathbf{e}_i$ is occupied, and zero otherwise ($\mathbf{e}_i$ is the unit vector in direction i). Close-packed hard-core dimers obey the condition $\sum_i n_i(\mathbf{x}) + n_i(\mathbf{x} - \mathbf{e}_i) = 1$.

On a bipartite lattice, each dimer touches one site on each sublattice (cf. Fig. 1, where the two sublattices are indicated by light and dark dots). Using a sublattice sign factor $\sigma_{\mathbf{x}} = \pm 1$ depending on whether the site $\mathbf{x}$ belongs to one or the other sublattice, we can now define a field variable on each link

$$B_i(\mathbf{x}) = \sigma_{\mathbf{x}}[n_i(\mathbf{x}) - z^{-1}] \tag{1}$$

(where z is the coordination number) as shown in Fig. 1. For close-packed dimers the lattice divergence of the field $\mathbf{B}$ vanishes, $\sum_i B_i(\mathbf{x}) - B_i(\mathbf{x} - \mathbf{e}_i) = 0$; i.e., $\mathbf{B}$ is a lattice

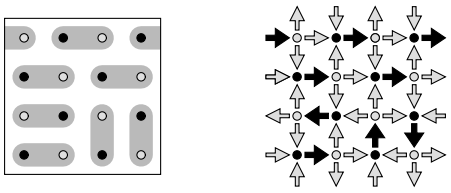

FIG. 1. Dimer configuration on the bipartite square lattice (left) and corresponding configuration of the divergence-free magnetic field (right—a dark arrow carries 3 times the flux of a light one). The two lower quadrants represent plaquettes which can be flipped (dimers rotated by $\pi/2$). These plaquettes have zero average $\mathbf{B}$ field.

magnetic field without monopoles. A monomer is a monopole with charge ± 1 depending on the sublattice.

We define the lattice flux ϕ_Σ through a surface Σ which does not contain any sites as the sum of the magnetic fields on the links piercing it $\phi_\Sigma = (\iint \mathbf{B} \cdot \mathbf{dS})_{\text{lattice}}$. For a cube with periodic boundary conditions, the flux through any surface that wraps around the system is invariant under local rearrangements of the dimers and under lattice translations of the surface. In particular, if we let Σ_i be planes perpendicular to the cubic unit vectors $\mathbf{e}_i$, the fluxes Φ_i through them are the maximal invariants that characterize a given topological sector of the dimer model. For an L^3 cube the maximal possible flux is $L^2/2$.

A dimer configuration may be represented by a lattice magnetic field in any dimension. In 2D, one solves the constraint $\nabla \cdot \mathbf{B} = 0$ through $\mathbf{B} = \nabla \times h$ [16], where h, the height function mentioned earlier, is a scalar field on the dual lattice. In 3D, $\mathbf{B}$ is computed from a vector potential $\mathbf{A}$ on the links of the dual lattice. Given an arbitrary $\mathbf{A}$ we recover $\mathbf{B}$ as its (lattice) curl, $\mathbf{B} = \nabla \times \mathbf{A}$ which is computed as

$$B_i(\mathbf{x}) = \sum_{\mathbf{y} \in \partial p} A_j(\mathbf{y}), \tag{2}$$

the oriented sum of the link variables on the boundary ∂p of the dual plaquette $p_i(\mathbf{x})$ pierced by the link $(\mathbf{x}, \mathbf{x} + \mathbf{e}_i)$. While in 2D, h is defined up to a global constant, in 3D, we have local gauge transformations, $A_j(\mathbf{y}) \to A_j(\mathbf{y}) + \Lambda(\mathbf{y} + \mathbf{e}_j) - \Lambda(\mathbf{y})$, where Λ is an arbitrary function on the sites of the dual lattice. Consequently, it is necessary to pick a gauge to work out properties of the $\mathbf{A}$. The fluxes Φ_i can be computed from the lattice line integrals of the vector potential along the boundaries of Σ_i. Hence the sector with all $\Phi_i = 0$ is obtained from gauge fields $\mathbf{A}$ that obey periodic boundary conditions themselves.

In analogy to 2D we now conjecture that the long-wavelength fluctuations of $\mathbf{A}$ and therefore $\mathbf{B}$ are governed by a probability distribution for the coarse-grained fields:

$$P[\mathbf{A}] \propto e^{-(K/2)\int_V (\nabla \times \mathbf{A})^2} \equiv e^{-(K/2)\int_V \mathbf{B}^2} \tag{3}$$

in the vicinity of the zero flux $\Phi_i = 0$ state. In the exponent of Eq. (3) the energy $\mathbf{B}^2/2$ of a magnetic field appears naturally. Configurations that locally minimize the (coarse-grained) field strength (cf. the lower quadrants of Fig. 1) maximize the number of flippable plaquettes with two parallel dimers and have high entropy, as described by Eq. (3).

Two comments are in order:

(i) The assertion Eq. (3) implies that the gauge field is in a Coulomb phase, in the language of lattice gauge theories. The existence of this phase in our lattice system is not in conflict with Polyakov's proof of confinement [17] for the standard U(1) lattice gauge theory in 3D because in our case the microscopics explicitly forbid the monopoles that were crucial to his analysis.

(ii) Gauge invariance explictly forbids any relevant operators at the fixed point defined by Eq. (3); this is the standard explanation of the masslessness of the photon. Consequently, the prediction of a Coulomb phase is self-consistent and weak perturbations cannot give rise to anything new. This should be contrasted with the situation in 2D, where vertex operators can become relevant even at weak coupling and, depending on the height stiffness and the radius of the height field, lead to a flat phase instead of the rough phase described by a purely Gaussian action.

Returning to the ansatz (3) it is straightforward to deduce the long distance correlator,

$$\langle B_i(\mathbf{x}) B_j(0) \rangle = \frac{1}{4\pi K} \frac{3x_i x_j - r^2 \delta_{ij}}{r^5}, \tag{4}$$

which is of the standard 3D dipole form. Reinserting the sublattice sign factors gives the connected dimer correlators.

To test the dipole form, we have carried out Monte Carlo simulations using the pocket algorithm [7,18] on large cubic lattices of size L^3 with L up to 128, with periodic boundary conditions. We have computed the connected correlation function for dimers at site $\mathbf{x}$ and at $\mathbf{x} + \mathbf{r}$, both pointing in the same direction $\mathbf{e}_1 = [100]$. The vector $\mathbf{r}$ was taken as a multiple of lattice vectors [111], [010], [100], [110]. The correlations nicely fall off as $1/r^\zeta$ in the regime $a \ll r \ll L$, with ζ close to 3. Furthermore, the ratios of the correlations also agree very well with the predicted dipole form Eq. (4), as shown in Fig. 2.

Going beyond this regime, we can even compute the scaling form of the correlations for $r \sim L$ through a proper treatment of the periodic boundary conditions used by our algorithm, which explores all topological sectors. In the long-wavelength description, we can write the fields in a given flux (topological) sector as $\mathbf{B}(\mathbf{x}) = \sum_i (\Phi_i/L^2)\mathbf{e}_i + \mathbf{B}'(\mathbf{x})$ so that the field $\mathbf{B}'$ now carries zero flux. When $\mathbf{\Phi} = \sum_i \Phi_i \mathbf{e}_i$ is nonzero, the stiffnesses $K_\parallel$ and $K_\perp$ for fluctuations parallel and perpendicular to it will

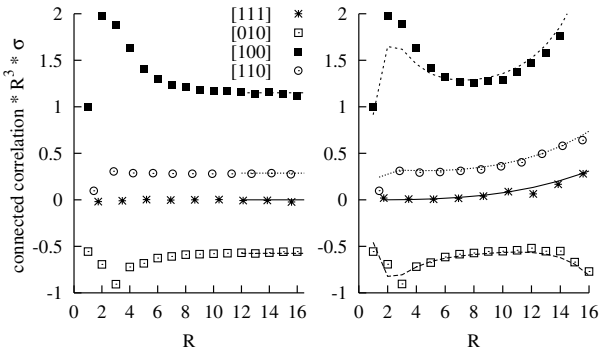

FIG. 2. Monte Carlo data of connected correlations (symbols) between parallel dimers, $z^2\langle n_i(\mathbf{x})n_i(0)\rangle - 1$, in various directions, multiplied by the sublattice sign factor $\sigma_{\mathbf{x}}$ and by R^3, plotted vs the Euclidean distance between the dimers, R. The coordination $z = 6$ for the cubic lattice. Left: for a system of size $L = 128$, $R \ll L$, the dipolar asymptotes are indicated by horizontal lines. The overall scale factor is fixed by normalizing those lines with respect to the [100] correlations. Right: for a system size $L = 32$, the data are compared to our finite-size formula; the only fitting parameter is an overall scale factor.

no longer be equal. Nevertheless, these are semimicroscopic and hence can depend only on the average local magnetic field. Consequently, we expect that both $K_{\parallel,\perp} = K + O(\Phi^2/L^4)$, where K is the stiffness in the zero flux sector.

With these considerations we can generalize (3) to

$$P[\mathbf{B}] \propto e^{-(K_\parallel/2)(\Phi^2/L)} e^{-1/2\int_V (K_\parallel B_\parallel'^2 + K_\perp B_\perp'^2)}. \qquad (5)$$

The first factor will ensure that $\Phi \sim O(\sqrt{L})$ whence $K_{\parallel,\perp} = K + O(1/L^3)$ so that the stiffness anisotropy can be ignored for large systems.

We can now deduce the correlations in a given flux sector, $\langle B_i(\mathbf{x})B_j(0)\rangle_{\mathbf{\Phi}} = \Phi_i\Phi_j/L^4 + \langle B_i'(\mathbf{x})B_j'(0)\rangle$ where the second piece is independent of $\mathbf{\Phi}$. After averaging the first term with weight $e^{-(K/2)(\Phi^2/L)}$, it equals $\delta_{ij}/(KL^3)$. From dimensional analysis we know that the second piece is of the form $f_{ij}(\mathbf{x}/L)/(KL^3)$ so that the two terms together have the appropriate form for a finite-size scaling function.

Finally, we have also determined the correlator $\langle B_i'(\mathbf{x})B_j'(0)\rangle$ in a finite-sized sample subject to periodic boundary conditions. We are not aware of a closed form evaluation of this quantity but can write it as a sum in momentum space, which needs ultraviolet regularization. As we eventually compare it to a lattice simulation, it is most convenient to do this via a lattice sum The resulting forms, e.g., $\langle B_x(\mathbf{m}a)B_x(0)\rangle = \mathcal{L}/(KL^3)$ with $\mathcal{L}$ given by

$$1 + \sum_{\mathbf{n}\neq\mathbf{0}} \frac{[4 - 2\cos(2\pi a n_y/L) - 2\cos(2\pi a n_z/L)]}{[6 - 2\sum_i \cos(2\pi a n_i/L)]} e^{i2\pi a \mathbf{n}\cdot\mathbf{m}/L},$$

can then be compared directly with the simulations' results for distances large compared to a lattice constant, a. In Fig. 2, the results are shown for a system of size $L = 32$. After adjusting the one free parameter to $Ka^3 = 4.9$ the curves agree well with simulation data for r larger than a few lattice spacings. A more detailed finite-size analysis that lets the exponent ζ vary finds it to be $\zeta = 3.00 \pm 0.02$, in excellent agreement with the dipolar form.

The gauge representation can be used to compute other operators of interest. Most notably, it shows that the interaction between two monomers is an attractive entropic force with the same form as that between oppositely charged monopoles, i.e., an inverse squared force. One can also consider the Wilson loop $\langle \exp(i\int_C \mathbf{A}\cdot d\mathbf{l})\rangle$ along a closed contour C. In the deconfined phase this exhibits a perimeter law at large loop sizes; i.e., it decays as e^{-P}, where P is the perimeter of the loop C, although with interesting corrections coming from the long range nature of the Coluomb force [19].

fcc lattice.—As was emphasized above, we expect a fundamental distinction between bipartite and nonbipartite dimer models. For the latter, the lack of a gauge representation indicates the absence of a Coulomb phase. To investigate this, we have simulated dimers on the face-centered cubic lattice, a simple nonbipartite 3D Bravais lattice.

In Fig. 3, we display the connected correlations between two parallel dimers in two different directions on a system of size $L = 10$, i.e., containing 4×10^3 sites. The decay of the oscillating correlations is *extremely* rapid and fits well to an exponential form with a correlation length of $\xi = 0.35 \pm 0.01$ nearest neighbor distances. This establishes that the fcc dimer model is in an exponentially deconfined phase.

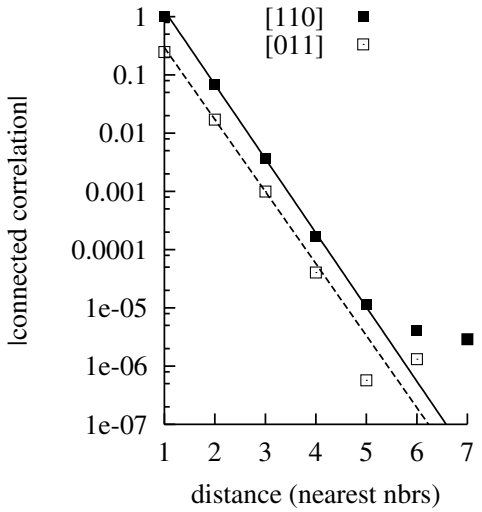

FIG. 3. Monte Carlo data for normalized connected dimer correlations, $|144\langle n_i(\mathbf{x})n_i(0)\rangle - 1|$ on the $L = 10$ fcc lattice, for i along the [110] direction. Separations $\mathbf{x}$ are along [110] and [011] and are measured in nearest-neighbor spacings, as indicated.

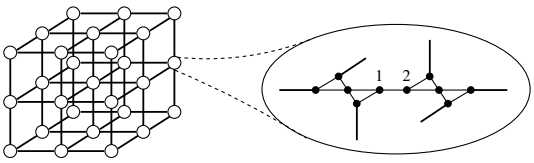

FIG. 4. The 3D Fisher lattice is obtained by decorating the sites of a simple cubic lattice (left) with the cluster shown on the right. Its six external legs (heavy lines) correspond to the original bonds of the cubic lattice. The numbers denote the possible locations of the test monomers.

Fisher lattice.—It is also possible to identify a 3D dimer model with exponential correlations and both confined and deconfined phases analytically. This is done by mapping the 3D Ising magnet on the cubic lattice onto a dimer model on the decorated cubic lattice shown in Fig. 4, where the original bonds have fugacity $z = 1/\tanh K$ (K being the strength of the ferromagnetic coupling), whereas those internal to the decorating clusters have fugacity 1. The correlator of the cubic Ising model between spins S_i, S_j at sites i and j can be expressed in terms of monomer correlators of the resulting dimer model in the same way as described in detail in Ref. [11] for the corresponding 2D lattice [10]—in fact, the analysis carries over to any dimension.

One obtains $\langle S_i S_j \rangle = \sum_{k_i,k_j=1}^{2} m_{(i,k_i),(j,k_j)}$, where $m_{(i,k_i),(j,k_j)}$ denotes the correlator of test monomers located on sites k_i of cluster i and k_j of cluster j (see Fig. 4). This correlator is given by the ratio of the partition functions with and without the pair of monomers present.

In the high temperature phase of the Ising model, $\langle S_i S_j \rangle \to 0$ exponentially, so that all monomer pairs are confined. At low temperatures $\langle S_i S_j \rangle$ decays exponentially to a constant. Therefore, at least one pair of monomers is deconfined. Unless possible algebraic terms present in the four correlators exactly cancel, which seems very unlikely, the deconfinement is exponential.

Conclusions.—We have argued that the distinction between the behavior of bipartite and nonbipartite lattices familiar from dimer models in 2D holds also in 3D. The former are characterized by a conservation law in a long-wavelength description which gives us a Coulomb phase in 3D and *mutatis mutandis* should do so in all $d > 3$ as well. Nonbipartite lattices lack such a constraint and can be generically expected to exhibit exponentially confined or deconfined phases as they do in our 3D examples. The Coulomb phase should also arise in other problems that involve conservation laws, e.g., the statistical mechanics of spin ice which is also the Ising antiferromagnet on the pyrochlore lattice [20]. Finally, we note that Hermele, Fisher, and Balents [21] are considering a set of closely related three-dimensional models.

R. M. thanks Leon Balents, Matthew Fisher, and Mike Hermele for several useful discussions. R. M. was in part supported by the Ministère de la Recherche et des Nouvelles Technologies with an ACI grant, and thanks the KITP for hospitality during part of this work. The NSF supported this work via PHY-9907949 (KITP), DMR-9978074 (S. L. S.), and DMR-0213706 (D. A. H. and S. L. S.). S. L. S. acknowledges support by the David and Lucile Packard Foundation.

[1] R. Kenyon, "An Introduction to the Dimer Model," available at http://topo.math.u–psud.fr/~kenyon/papers/dimers.ps.Z
[2] J. Nagle, C. S. O. Yokoi, and S. M. Bhattacharjee, in *Phase Transitions and Critical Phenomena*, edited by C. Domb and J. Lebowitz (Academic Press, London 1989), Vol. 13.
[3] F. Y. Wu, cond-mat/0303251.
[4] M. Udagawa, M. Ogata, and Z. Hiroi, J. Phys. Soc. Jpn. **71**, 2365 (2002); R. Moessner and S. L. Sondhi, Phys. Rev. B **68**, 064411 (2003).
[5] P. W. Kasteleyn, Physica (Utrecht) **27**, 1209 (1961); J. Math. Phys. (N.Y.) **4**, 287 (1963).
[6] M. E. Fisher and J. Stephenson, Phys. Rev. **132**, 1411 (1963).
[7] W. Krauth and R. Moessner, Phys. Rev. B **67**, 064503 (2003).
[8] P. Fendley, R. Moessner, and S. L. Sondhi, Phys. Rev. B **66**, 214513 (2002).
[9] G. Misguich, D. Serban, and V. Pasquier, Phys. Rev. Lett. **89**, 137202 (2002).
[10] M. E. Fisher, J. Math. Phys. (N.Y.) **7**, 1776 (1966).
[11] R. Moessner and S. L. Sondhi, Phys. Rev. B **68**, 054405 (2003).
[12] H. W. J. Blöte and H. J. Hilhorst, J. Phys. A **15**, L631 (1982); B. Nienhuis, H. J. Hilhorst, and H. W. Blöte, *ibid.* **17**, 3559 (1984).
[13] C. L. Henley, J. Stat. Phys. **89**, 483 (1997).
[14] R. Moessner and S. L. Sondhi, cond-mat/0307592 [Phys. Rev. B (to be published)].
[15] D. S. Rokhsar and S. A. Kivelson, Phys. Rev. Lett. **61**, 2376 (1998).
[16] R. Youngblood, J. D. Axe, and B. M. McCoy, Phys. Rev. B **21**, 5212 (1980).
[17] A. M. Polyakov, Nucl. Phys. **B120**, 429 (1977).
[18] C. Dress and W. Krauth, J. Phys. A **28**, L597 (1995).
[19] J. B. Kogut, Rev. Mod. Phys. **51**, 659 (1979).
[20] C. L. Henley (unpublished).
[21] M. Hermele, M. P. A. Fisher, and L. Balents, cond-mat/0305401.